JACS
JOURNAL OF THE AMERICAN CHEMICAL SOCIETY

Article

pubs.acs.org/JACS

A Facile Multi-interface Transformation Approach to Monodisperse Multiple-Shelled Periodic Mesoporous Organosilica Hollow Spheres

Zhaogang Teng,[†,‡,#] Xiaodan Su,[§,#] Yuanyi Zheng,[†] Junjie Zhang,[§] Ying Liu,[†] Shouju Wang,[†] Jiang Wu,[†] Guotao Chen,[†] Jiandong Wang,[†] Dongyuan Zhao,*[,⊥] and Guangming Lu*[,†,‡]

[†]Department of Medical Imaging, Jinling Hospital, School of Medicine, Nanjing University, Nanjing 210002, Jiangsu, P.R. China

[‡]State Key Laboratory of Analytical Chemistry for Life Science, School of Chemistry and Chemical Engineering, Nanjing University, Nanjing 210093, Jiangsu, P.R. China

[§]Key Laboratory for Organic Electronics & Information Displays and Institute of Advanced Materials, Nanjing University of Posts and Telecommunications, Nanjing 210046, Jiangsu, P.R. China

[⊥]Department of Chemistry, Laboratory of Advanced Materials, Shanghai Key Laboratory of Molecular Catalysis and Innovative Materials, Fudan University, Shanghai 200433, P.R. China

Supporting Information

ABSTRACT: The synthesis of well-defined and complex hollow structures via a simple method is still a major challenge. In this work, a facile and controllable "multi-interface transformation" approach for preparation of monodisperse multi-shelled periodic mesoporous organosilica (PMO) hollow spheres has been established by a one-step hydrothermal treatment of successively grown organosilica particles. The multi-shelled PMO hollow spheres have inorganic−organic hybrid frameworks, controllable number (1−4) of shells, high surface area (~805 m^2/g), accessible ordered mesochannels (~3.2 nm), large pore volume (1.0 cm^3/g), and uniform and tunable diameter (300−550 nm), chamber size (4−54 nm), and shell thickness (10−30 nm). In addition, various organic groups (alkyl, aromatic, and heteroelement fragments) are successfully incorporated into the multi-shelled PMO hollow spheres by successively adding different bridged organosilica precursors. Notably, the distribution of different kinds of organic groups in the multi-shelled PMO hollow spheres can be precisely controlled, showing great potential for future applications. We propose that the formation of the multi-shelled PMO hollow structures is ascribed to the creation of multiple highly cross-linked organosilica interfaces, providing a new and interesting fundamental principle for PMO materials. Due to their unique structure and frameworks, triple-shelled ethane-bridged PMO hollow spheres were successfully loaded with an anti-cancer drug doxorubicin and perfluoropentane gas, which present excellent effects in the killing of cancer cells and ultrasound imaging. It is expected that the multi-interface transformation strategy provides a simple, controllable, versatile, and template-free method for preparation of various multifunctional PMOs for different applications.

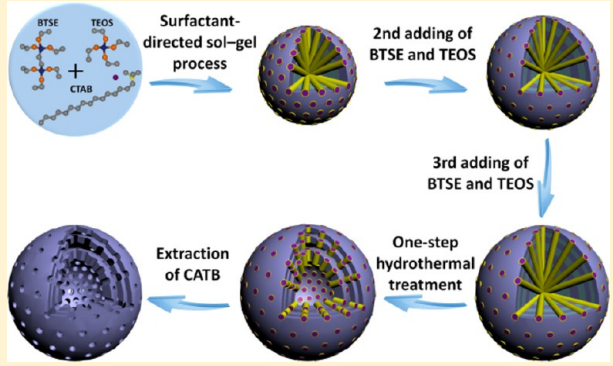

1. INTRODUCTION

Hollow micro- and nanoscale particles have recently been subjected to extensive research because of their unique characteristics, such as low density, high surface area, and large interior space, and their potential applications in various fields.[1−7] More recently, considerable effort has been devoted to the fabrication of hollow particles with multiple shells to endow the structures with more heterogeneous interfaces, compartmentation environments, and thus better physicochemical properties, such as prolonged drug release, enhanced catalytic activity, and improved energy conversion and storage capacity.[8−18]

Conceptually, multi-shelled structures can be prepared by the layer-by-layer templating approach, which involves alternating deposition of designed and sacrificial materials onto preformed particles and then removal of the templates via dissolution or calcination.[19−21] However, this synthetic method is challenging, since the multi-step deposition and template removal procedures are tedious, time-consuming, and uneconomic. Some other strategies based on multi-lamellar vesicle templating,[22−24] Ostwald ripening,[25,26] redox etching,[27] ionic exchange reaction,[9,28] and thermal treatment of metal ions containing polymer/carbon spheres[12−16,29,30] have also been developed to fabricate the multi-shelled hollow structures. However, control over the size distribution, morphological uniformity, chamber volume, clarity of the shells, and functional groups of the products by these approaches is generally less

Received: May 23, 2015
Published: June 1, 2015

DOI: 10.1021/jacs.5b05369
J. Am. Chem. Soc. 2015, 137, 7935−7944

feasible due to the complexity of the hierarchical structures. Furthermore, the shells of the multi-shelled structures prepared by these methods do not possess ordered permeable mesochannels. As a result, they are not favorable for adsorption and release of reactants or guest molecules and thus limited in catalysis, biomedicine, and other applications. In addition, the shells are generally composed of inorganic materials or organic materials (such as metal oxides or polymers). Multi-shelled hollow spheres with inorganic−organic hybrid frameworks have not been reported, even though the integration of organic and inorganic fragments can endow the hybrid materials with more colorful properties for different applications.[31,32]

Periodic mesoporous organosilicas (PMOs) created by surfactant-directed self-assembly represent a promising class of inorganic−organic hybrid materials since they possess accessible ordered mesopores, large surface areas, organic-group-incorporated frameworks, and mechanical and hydrothermal stability.[33,34] A number of PMO materials have been successfully prepared with different organic components, mesostructures, and morphologies, providing potential applications in many areas.[35−41] However, the differences in the PMOs' frameworks at different reaction stages has rarely been considered due to the fast hydrolysis and condensation processes of precursors and difficulty in directly analyzing the resultant materials on a molecular scale. A deep understanding of this issue is important not only from the fundamental aspect but also for providing new approaches to PMOs with a high degree of architectural complexity yet highly controlled morphologies and structures.

Herein, we demonstrate a simple multi-interface transformation approach to prepare monodisperse multiple-shelled PMO hollow spheres by taking advantages of multiple high-cross-linking organosilica interfaces formed at later reaction stages in ammonia and ethanol solution. The method involves successive growth of mesostructured organosilica spheres via cetyltrimethylammonium bromide-directed sol−gel processes followed by a one-step hydrothermal treatment, during which a solid-to-hollow transformation occurs, accompanied by formation of multiple interfaces. The multi-shelled PMO hollow spheres obtained possess a controllable number (1−4) of shells, highly uniform and tunable diameter (300−550 nm), chamber size (4−54 nm), and shell thickness (10−30 nm), high surface area (~805 m^2/g), accessible ordered radial mesochannels (~3.2 nm), large pore volume (1.0 cm^3/g), and also inorganic−organic hybrid frameworks. Moreover, multi-shelled PMO hollow spheres with different organic groups (alkyl, aromatic, or heteroelement fragments) on each shell are facilely synthesized by the method. As a proof of concept, we show that the multi-shelled PMO hollow spheres possess good biocompatibility and can be used to load anti-cancer drugs doxorubicin (DOX) and perfluoropentane (PFP) gas, respectively, for killing of human breast adenocarcinoma cells and ultrasound imaging.

2. EXPERIMENTAL SECTION

2.1. Materials. Tetraethoxysilane (TEOS), cetyltrimethylammonium bromide (CTAB), concentrated ammonia aqueous solution (25 wt%), anhydrous ethanol, and $HAuCl_4{\cdot}4H_2O$ were purchased from Sinopharm Chemical Reagent Co., Ltd. (Shanghai, China). 1,2-Bis(triethoxysilyl)ethane (BTSE), 1,4-bis(triethoxysily)propane tetrasulfide (TESPTS), and 1,4-bis(triethoxysily)benzene (BTSB) were bought from Sigma-Aldrich (St. Louis, MO, USA). Millipore water with a resistivity of 18.2 MΩ cm was used in all experiments.

2.2. Preparation of Ethane-Bridged Multi-shelled PMO Hollow Spheres. Mesostructured organosilica spheres were first prepared via a surfactant-directed sol−gel process in ethanol aqueous solution containing CTAB, TEOS, BTSE, and ammonia. In brief, CTAB (0.16 g) was dissolved in a mixed solution of ethanol (30 mL), water (75 mL), and concentrated ammonia aqueous solution (1.0 mL, 25 wt%). After this solution was stirred at 35 °C for 1 h, a mixture of silane precursors (BTSE and TEOS) was rapidly added under vigorous stirring (1100 rpm). The molar ratio of the reaction mixture was 1.00 TEOS:0.604 BTSE:0.787 CTAB:23.6 NH_3:7455 H_2O:921 C_2H_5OH. The resultant mixture was stirred at 35 °C for 24 h, after which the white reaction product was further successively coated with mesostructured organosilica layers. Typically, a mixture of TEOS (0.125 mL) and BTSE (0.125 mL) was rapidly added to the suspension under vigorous stirring (1100 rpm). After stirring at 35 °C for 24 h, two-layered mesostructured organosilica spheres were obtained. Following the preparation procedure and the same experimental conditions described above, the organosilicas were deposited with the desired number of layers. The obtained multi-layered organosilica spheres were then collected by centrifugation and washed with ethanol. To carry out the multi-interface transformation, the mesostructured organosilica spheres were re-dispersed in water to a final concentration of 0.5 mg mL^{-1} and transferred to Teflon-lined stainless-steel autoclaves. The autoclaves were further heated in an air-flow electric oven at 120 °C for 5 h. Afterward, the autoclaves were cooled to room temperature, and the products were collected by centrifugation. Finally, CTAB templates were removed from the products by three solvent extractions in a solution containing ethanol (180 mL) and concentrated HCl (360 μL, 37%) at 60 °C for 3 h. After the extracts were washed with ethanol three times and dried under a high vacuum, multi-shelled PMO hollow spheres were obtained.

2.3. Preparation of Double-Shelled Thioether- and Ethane-Bridged PMO Hollow Spheres. First, mesostructured thioether-bridged organosilica spheres were prepared. In brief, CTAB (0.08 g) was dissolved in a mixed solution of ethanol (15 mL), water (37.5 mL), and concentrated ammonia aqueous solution (0.5 mL). After this solution was stirred at 35 °C for 1 h, a mixture of TESPTS (0.025 mL) and TEOS (0.0625 mL) was rapidly added under vigorous stirring. The resultant mixture was stirred at 35 °C for 24 h, after which the thioether-bridged product was collected and further coated with ethane-bridged organosilica layers. Typically, the thioether-bridged organosilicas were re-dispersed in a mixture containing CTAB (0.16 g), ethanol (30 mL), water (75 mL), and concentrated ammonia aqueous solution (1.0 mL). After ultrasonic dispersion for 2 h and further stirring at 35 °C for 1 h, a mixture of TEOS (0.125 mL) and BTSE (0.125 mL) was rapidly added to the suspension. After stirring at 35 °C for 24 h, thioether- and ethane-bridged organosilica spheres were obtained. The obtained organosilica spheres were then re-dispersed in 450 mL of water and hydrothermally treated at 180 °C for 12 h. After removal of the surfactant template by HCl/ethanol extraction, double-shelled thioether- and ethane-bridged PMO hollow spheres were obtained. The double-shelled thioether- and ethane-bridged PMO hollow spheres (8 mg) were then incubated with 7 mL of $HAuCl_4{\cdot}4H_2O$ (0.014 M) aqueous solution at room temperature for 12 h, and EDX mapping was carried out to observe the absorption position of the precious metal ions in the particles.

2.4. Characterization. Transmission electron microscopy (TEM) images were obtained by using an HT7700 microscope (Hitachi, Tokyo, Japan) operated at 100 kV accelerating voltage, a JEOL 2100F microscope (Japan) at 200 kV, or a Talos F200X microscope (FEI, Hillsboro, OR, USA) at 200 kV. Energy-dispersive X-ray (EDX) and high-angle annular dark-field scanning TEM (HAADF-STEM) analyses were performed with a FEI Talos F200X electron microscope at 200 kV with an EDX detector system. The samples for TEM and EDX measurements were suspended ultrasonically in ethanol and supported onto a carbon-coated copper grid. Scanning electron microscopy (SEM) images were taken on a Hitachi S4800 microscope (Tokyo, Japan) operated at 3−5 kV and 10 μA. FT-IR spectra were collected on a Nicolet NEXUS870 spectrometer (Nicolet Instruments Inc., Madison, WI, USA), using KBr pellets of the solid samples. ^{29}Si

DOI: 10.1021/jacs.5b05369
J. Am. Chem. Soc. 2015, 137, 7935−7944

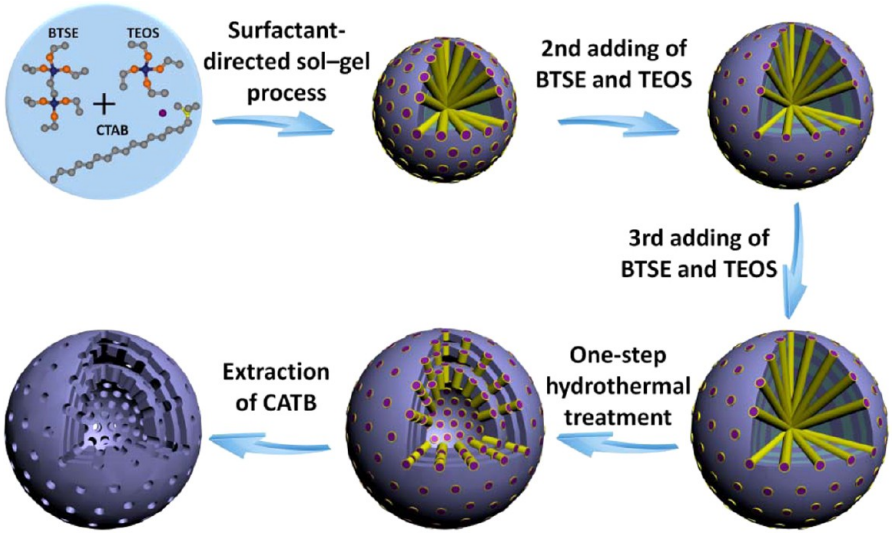

Figure 1. Illustration of the preparation of triple-shelled PMO hollow spheres by the multi-interface transformation approach.

magic-angle spinning (MAS) NMR spectra were recorded at 79.48 MHz on a Bruker AVIII400 spectrometer with a 7 mm MAS, using a spinning rate of 6.0 kHz and a recycle delay of 120 s. The chemical shifts were referenced to 3-(trimethylsilyl)-1-propanesulfonic acid sodium salt (DSS). X-ray power diffraction (XRD) patterns were obtained with an ARL X'tra diffractometer with Cu Kα radiation (0.154 nm) operated at 40 kV and 40 mA. Nitrogen adsorption–desorption isotherms were measured using a Micromeritics ASAP 2020 analyzer at −196 °C. Before the measurements, the samples were degassed under vacuum at 150 °C for at least 10 h. The specific surface area (S_{BET}) was calculated with the Brunauer–Emmett–Teller (BET) method by using the adsorption data in a relative pressure (p/p_0) range from 0.14 to 0.25. The pore size distribution was obtained by applying proper nonlocal density functional theory (NLDFT) methods from the adsorption branch of isotherms. The total pore volume (V_{total}) was evaluated from the adsorbed amount at a relative pressure (p/p_0) of 0.994. The dissolved silicon contents during the hydrothermal treatment were determined by inductively coupled plasma atomic emission spectroscopy (ICP-AES) using a Perkin-Elmer Optima-5300DV spectrometer (Perkin-Elmer, Inc., Waltham, MA, USA).

2.5. *In Vitro* Cytotoxicity Assay. Human embryo kidney 293 cells obtained from American Type Culture Collection (ATCC) were seeded into 96-well plates at a density of 1×10^4 cells per well and incubated for 24 h. Different concentrations of the triple-shelled ethane-bridged PMO hollow spheres dispersed in Roswell Park Memorial Institute (RPMI) 1640 medium were then added to the cell culture. After 24 h incubation, 10 μL of 3-(4,5-dimethylthiazol-2-yl)-2,5-diphenyltetrazolium bromide (MTT, 5.0 mg mL^{-1} in culture medium) was added and incubated for an additional 4 h. Afterward, the cell culture was replaced with 150 μL of dimethyl sulfoxide. Finally, the absorbance of each sample was measured on a microplate reader (BioTek Instruments, Winooski, VT, USA) at 570 nm. The cell viability (%) was calculated as (mean absorbance value of treated cells/mean absorbance value of control cells) × 100.

2.6. *In Vitro* Chemotherapeutic Effect of DOX-Loaded PMO Hollow Spheres. To load DOX molecules, 10 mg of the triple-shelled ethane-bridged PMO hollow spheres was dispersed in 10 mL of phosphate-buffered saline (PBS) containing 3 mg of DOX and stirred for 24 h under dark conditions. The DOX-loaded PMO hollow spheres were then collected by centrifugation and washed with PBS three times. The loading and washing solutions were kept to measure the DOX payloads. To study the chemotherapeutic effect of the DOX-loaded PMO hollow spheres, human breast adenocarcinoma MDA-MB-231 cells obtained from ATCC were seeded into 96-well plates at a concentration of 1×10^4 cells per well and allowed to grow for 24 h. Different concentrations of DOX-loaded PMO hollow spheres in RPMI 1640 medium were then added to the culture. After 48 h incubation, the cytotoxicity of the samples was evaluated by the MTT assay described above.

3. RESULTS AND DISCUSSION

The procedure for preparation of the multi-shelled ethane-bridged PMO hollow spheres is shown in Figure 1. First, the mesostructured ethane-bridged organosilica spheres were prepared via a CTAB surfactant-directed sol–gel process in an ethanol aqueous solution by using TEOS and BTSE as precursors. Afterward, a mixture of TEOS and BTSE was further added step-by-step into the reaction solution with a time interval of 24 h. The addition time of the silane precursors determines the number of the shells of the finally obtained multi-shelled PMO hollow spheres. The successively grown organosilica spheres were then hydrothermally treated at 120 °C for 5 h to carry out the solid-to-hollow structural transformation. After extraction of CTAB surfactants by acidic ethanol, multi-shelled PMO hollow spheres with ordered radial mesochannels could be obtained.

The TEM images indicate that the mesostructured ethane-bridged organosilica spheres prepared by one-time addition of TEOS and BTSE precursors have a uniformly spherical morphology and an average diameter of about 300 nm (Figure 2a1). Through successive addition of equivalent precursors into the reaction solution with a time interval of 24 h, the diameter of the organosilica spheres increases from 300 to 400 and then to 480 nm (Figure 2a1, b1, c1). Interestingly, these spheres can be completely convert into single-, double-, and triple-shelled hollow structures after the hydrothermal treatment at 120 °C for 5 h, as revealed by the reduced TEM contrast in their interiors and intermediate layers (Figure 2a2-a3, b2-b3, c2-c3). The number of the shells of the obtained multi-shelled hollow sphere structures is remarkably determined by the addition times of silane precursors. Simultaneously, the products possess uniform spherical morphology, monodisperse size distribution, smooth surface, and clear hollow spaces. The diameter and shell thickness of the single-shelled PMO hollow spheres are measured to be 300 and 24 nm, respectively (Figure 2a2 and a3). It is obvious that the shells of the hollow particles retain the original diameter compared with their parent particles (Figure 2a1). For the double- and triple-shelled hollow

DOI: 10.1021/jacs.5b05369
J. Am. Chem. Soc. 2015, 137, 7935–7944

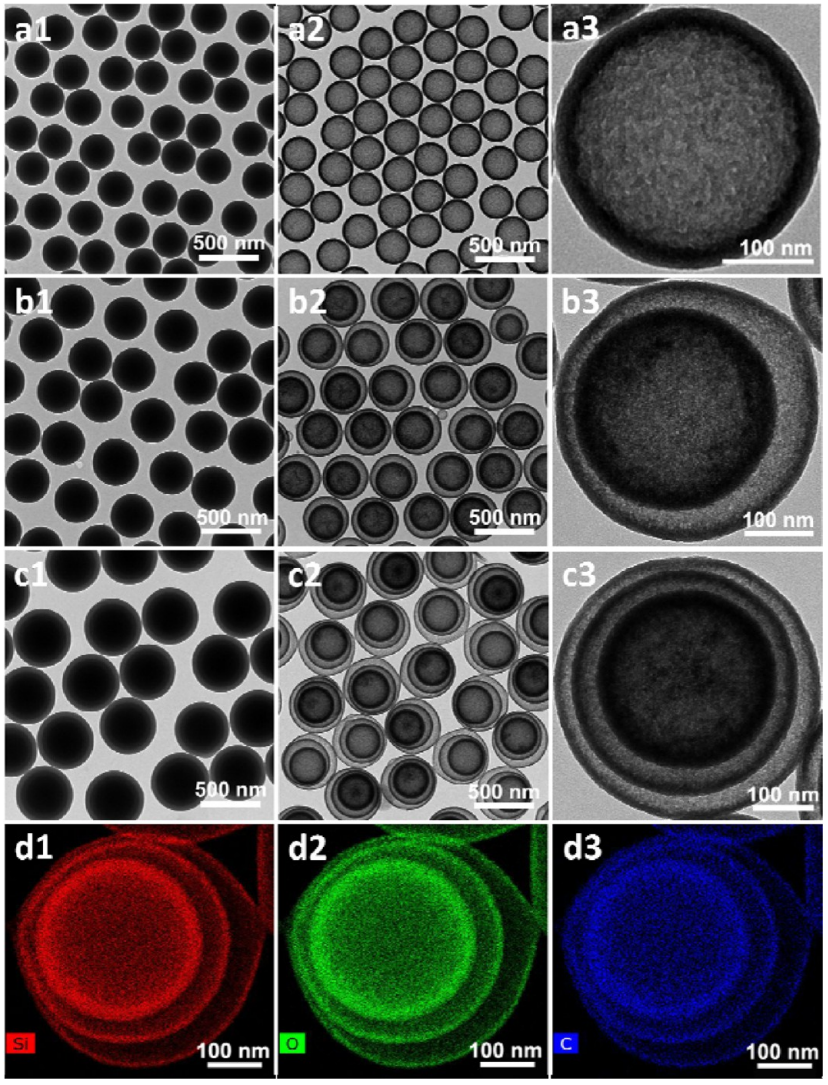

Figure 2. TEM images of the mesostructured organosilica spheres synthesized via a surfactant-directed sol−gel process in an ethanol aqueous solution by adding silane precursors (BTSE and TEOS) (a1) one, (b1) two, and (c1) three times. TEM images of (a2-a3) single-, (b2-b3) double-, and (c2-c3) triple-shelled PMO hollow spheres with ordered radial mesochannels prepared by a one-step hydrothermal treatment of the organosilica spheres with different growth cycles. (d1−d3) EDX elemental mapping images of the triple-shelled PMO hollow spheres. Red, green, and blue indicate silicon, oxygen, and carbon atoms, respectively.

structures, their internal shells are almost not located in the central positions of the sphere, as the large hollow spaces make them free (Figure 2b2-b3, c2-c3). The diameter and shell thickness of the double-shelled hollow spheres are 400 and 15 nm for the outer shells and 300 and 26 nm for the inner one (Figure 2b2-b3), respectively. The outer, intermediate, and inner shells of the triple-shelled structures have a diameter of 480, 400, and 300 nm, respectively, with a uniform thickness of 12, 17, and 29 nm (Figure 2c2-c3). It is remarkable that the diameter of the innermost shells of double- and triple-shelled PMO hollow spheres is identical to the diameter of the as-made mesostructured ethane-bridged organosilica spheres obtained by adding silane precursors one time. Simultaneously, the diameter of the intermediate shells of the triple-shelled structures is the same as that of the organosilicas formed by adding precursors two times. These results strongly indicate that the surface layers of the organosilicas synthesized with different addition cycles of silane precursors persist and form hollow shells with a certain diameter after the hydrothermal treatment. Simultaneously, ICP-AES measurements show that the dissolved silicon content after the hydrothermal treatment is only 19.4, 18.2, and 14.4% for the single-, double-, and triple-shelled PMO hollow spheres, respectively, suggesting that most silicate species are retained. The SEM images with different magnifications further reveal the uniform diameter and morphology of the products and their multi-shelled hollow structures (Supporting Information, Figure S1). Moreover, high-magnification TEM images show that the as-made mesostructured organosilicas and obtained multi-shelled PMO hollow spheres possess radially oriented mesopore channels with openings at the surface (Supporting Information, Figures S2 and S3), implying that the mesochannels are readily accessible for reactants or guest molecules and thus beneficial to confined reactions or drug delivery. The XRD pattern of the triple-shelled PMO hollow spheres shows a well-resolved diffraction peak at 2.1° (Supporting Information, Figure S4), indicating that the mesostructure is ordered. EDX elemental mapping performed on the triple-shelled PMO spheres shows that the Si, O, and C elements are uniformly distributed in the three-layer shells (Figure 2d1-d3 and Supporting Information,

DOI: 10.1021/jacs.5b05369
J. Am. Chem. Soc. 2015, 137, 7935−7944

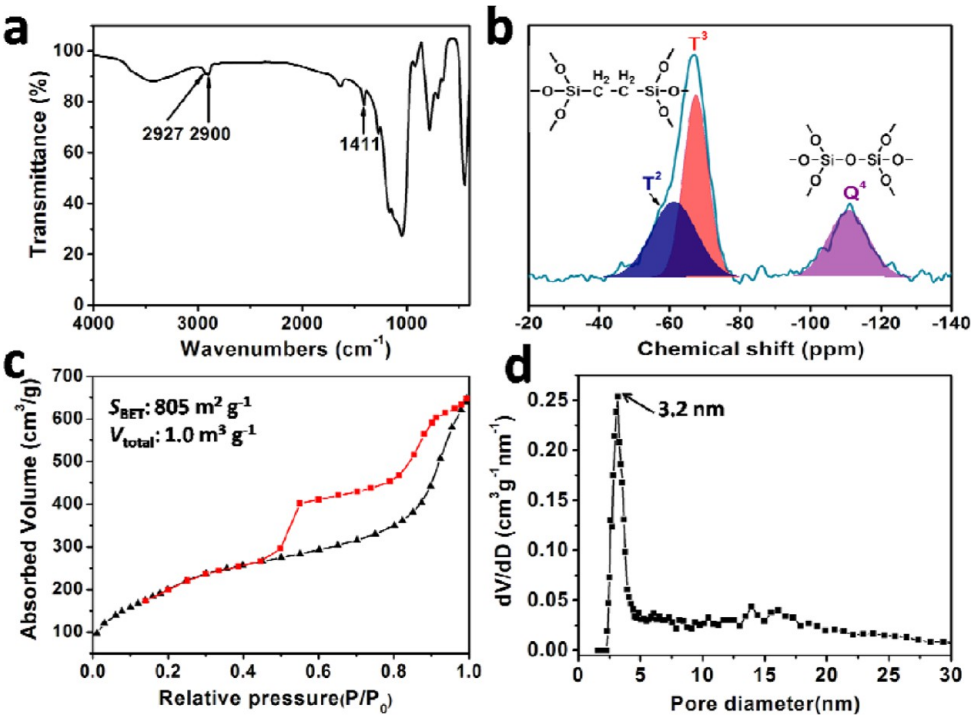

Figure 3. (a) FT-IR spectrum, (b) ^{29}Si MAS NMR spectrum, (c) nitrogen sorption isotherms, and (d) pore size distribution curve of the triple-shelled PMO hollow spheres prepared by the multi-interface transformation method after removal of the surfactant template by HCl/ethanol extraction.

Figure S5), suggesting uniform deposition of ethane-bridged silane in these shells. Furthermore, more complex quadruple-shelled PMO hollow spheres have also been successfully prepared by successively adding silane precursors four times (Supporting Information, Figure S6).

The composition of the multi-shelled PMO hollow spheres prepared by the multiple interface transformation approach was further confirmed by Fourier transform infrared (FT-IR) spectra and ^{29}Si MAS NMR. The FT-IR spectra of the triple-shelled PMO hollow spheres show absorbance bands at 2927, 2900, and 1411 cm^{-1} (Figure 3a), which can be assigned to the vibration of the C−H bond in the $-CH_2-CH_2-$ group, clearly indicating the ethane-bridged frameworks. The ^{29}Si MAS NMR spectrum of the triple-shelled PMO hollow spheres shows two sets of signals at −45 to −80 ppm and −95 to −125 ppm, corresponding to T^m ($C-Si(OSi)_m(OX)_{3-m}$, m = 1−3) and Q^n ($Si(OSi)_n(OX)_{4-n}$, X = H or Et, n = 1−4) species (Figure 3b). Quantitative analysis based on relative peak areas reveals that 74% of the silicon atoms in the triple-shelled PMO hollow spheres are located at the T sites, further indicating the inorganic−organic hybrid frameworks. Simultaneously, the overall condensation degree of the PMO frameworks is calculated to be as high as 89%. Nitrogen sorption isotherms of the triple-shelled PMO hollow spheres exhibit a type IV curve with a large hysteresis loop (Figure 3c), suggesting the mesoporous structure of the materials. The pore size distribution calculated using the NLDFT method further reveals that the spheres have a uniform mesopore size of 3.2 nm (Figure 3d). Besides, the surface area and pore volume of the triple-shelled PMO hollow spheres are calculated to be as high as 805 m^2 g^{-1} and 1.0 cm^3 g^{-1}, respectively.

The diameter, inter-shell spacings, and shell thickness of the multi-shelled PMO hollow spheres can be facilely and precisely modulated by controlling the CTAB concentration, amount of organosilica cores, and reaction temperature. TEM observations showed that the diameter of the triple-shelled PMO hollow spheres with well-defined structure decreased from 490 to 480 and then to 350 nm as CTAB concentration increased from 3.8 to 4.2 and 4.7 mmol L^{-1} (Figure 4a−c). Furthermore, we found that the mesostructured organosilica spheres formed in the ethanol aqueous solution could be isolated and re-dispersed into a new growth solution to prepare multi-shelled PMO hollow spheres with different inter-shell spacings. For example, double-shelled PMO hollow spheres with inter-shell spacings of 4, 18, and 54 nm can be prepared by simply decreasing the concentrations of organosilica cores from 1.9 to 1.1 and 0.5 mg mL^{-1} (Figure 4d−i). Furthermore, it was observed that the thickness of the outer shells of double-shelled PMO hollow spheres was decreased from 20 to 10 nm when the deposition temperature of the second organosilica layer decreased from 55 to 15 °C (Figure 5 and Supporting Information, Figure S7). It suggests that the shell thickness of the multi-shelled PMO hollow spheres can also be facilely and respectively controlled by adjusting the reaction temperature.

One of the salient features of PMO materials is that a huge variety of the bridged organic groups, such as alkyl, aromatic, or heteroelement moieties, can be introduced into the mesopore frameworks on molecular scales. Here, we demonstrate that the multi-interface transformation approach can also be extended to prepare multiple-shelled PMO hollow spheres with different organic groups on each shell. As an example, dual-bridged mesostructured organosilica spheres were prepared by coating an ethane-bridged organosilica layer on thioether-bridged organosilica particles (Figure 6a). Remarkably, the dual-bridged organosilica spheres could be completely transformed into double-shelled hollow spheres with a small core after hydrothermal treatment at 180 °C for 12 h (Figure 6b). To characterize the distribution of the ethane and the thioether

DOI: 10.1021/jacs.5b05369
J. Am. Chem. Soc. 2015, 137, 7935−7944

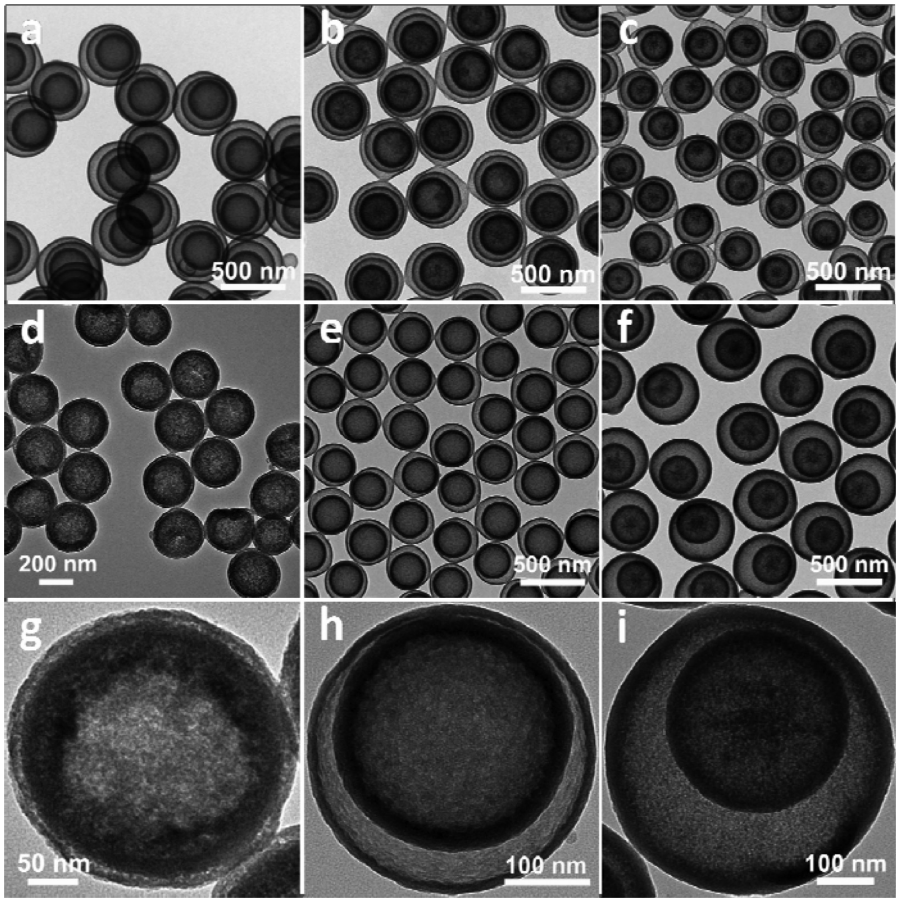

Figure 4. (a–c) TEM images of the triple-shelled PMO hollow spheres prepared via the multi-interface transformation method with CTAB concentrations of (a) 3.8, (b) 4.2, and (c) 4.7 mmol L^{-1}. (d–i) TEM images of the double-shelled PMO hollow spheres with a controllable inter-shell spacing as a function of the concentrations of the organosilica cores of (d,g) 1.9, (e,h) 1.1, and (f,i) 0.5 mg mL^{-1}.

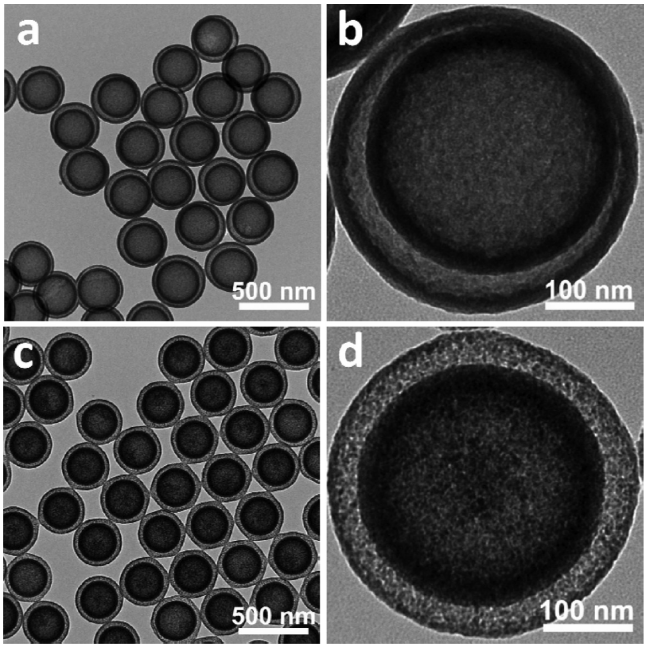

Figure 5. TEM images of the double-shelled PMO hollow spheres whose second shells are grown at (a,b) 55 and (c,d) 15 °C.

groups, the dual-bridged double-shelled hollow spheres were incubated with a solution of Au^{3+} (Figure 6c). The EDX elemental mapping results show that the Si, O, and C elements are present in the double shells and inner cores, clearly indicating the organosilica frameworks (Figure 6d–g). Notably, the S elements are mainly present in the inner yolk–shell spheres (Figure 6h), suggesting that the thioether groups from TESPTS are still located in the inner particles after the multi-interface transformation. Simultaneously, Au elements are also present in the inner yolk–shell particles due to the fact that the sulfur groups can bind with precious metal (Au) atoms via lone-pair electrons (Figure 6i). Furthermore, through coating an ethane-bridged organosilica layer on benzene-bridged organosilca particles and hydrothermal treatment at 100 °C, double-shelled benzene- and ethane-bridged PMO hollow spheres are also successfully prepared (Supporting Information, Figure S8). These results indicate that the multi-interface transformation approach is versatile for the preparation of multi-shelled hollow PMOs with different organic groups on each shell, providing great potential for controlled drug delivery, confined reaction, etc.

Based on the above results, it is directly realized that each surface of the organosilica/CTAB frameworks formed in the ammonia and ethanol solutions is retained and their corresponding interior disappears after the hydrothermal treatment. These facts strongly suggest that the surfaces and the interiors of the original organosilica/CTAB composites formed in the solutions are different in nature. To further verify this point, the organosilica/CTAB composite spheres synthesized via the CTAB-directed sol–gel process with different

DOI: 10.1021/jacs.5b05369
J. Am. Chem. Soc. 2015, 137, 7935–7944

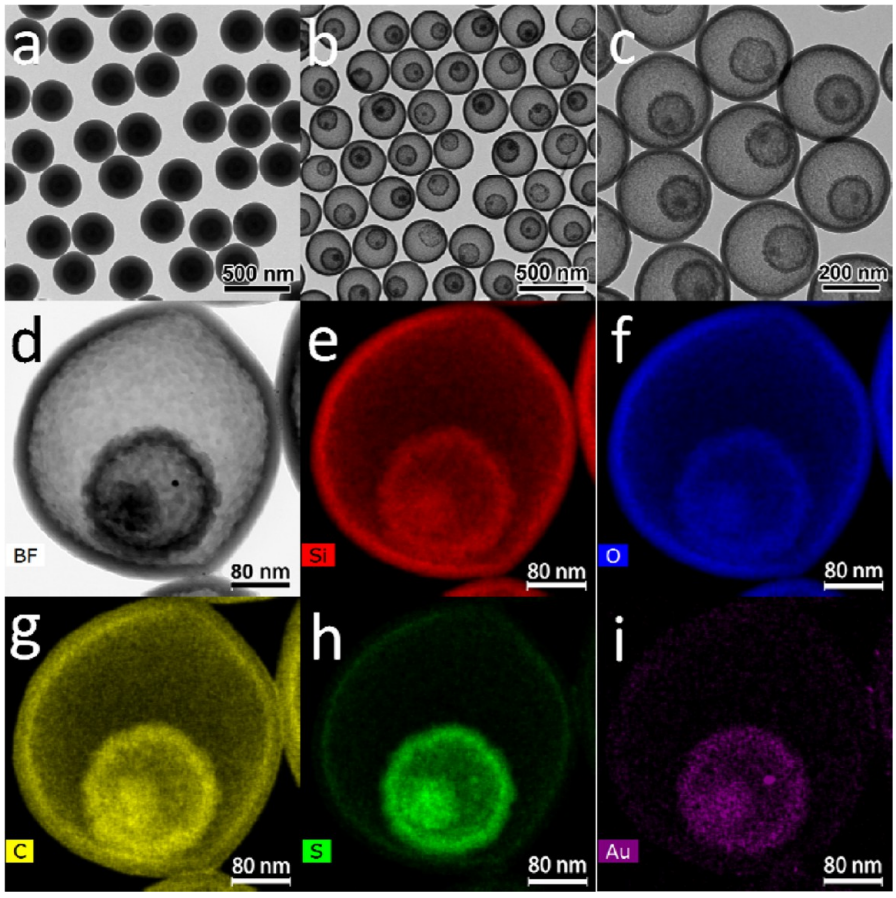

Figure 6. (a) TEM image of mesostructured organosilica spheres formed by coating an ethane-bridged organosilica layer on thioether-bridged organosilica particles. (b) TEM image of the double-shelled PMO hollow spheres formed by hydrothermal treatment of the dual-bridged spheres at 180 °C for 12 h. (c,d) TEM and (e–h) EDX elemental mapping images of the double-shelled thioether- and ethane-bridged PMO hollow spheres incubated with 0.014 M Au^{3+} solution. Red, blue, yellow, green, and purple indicate silicon, oxygen, carbon, sulfur, and gold atoms, respectively.

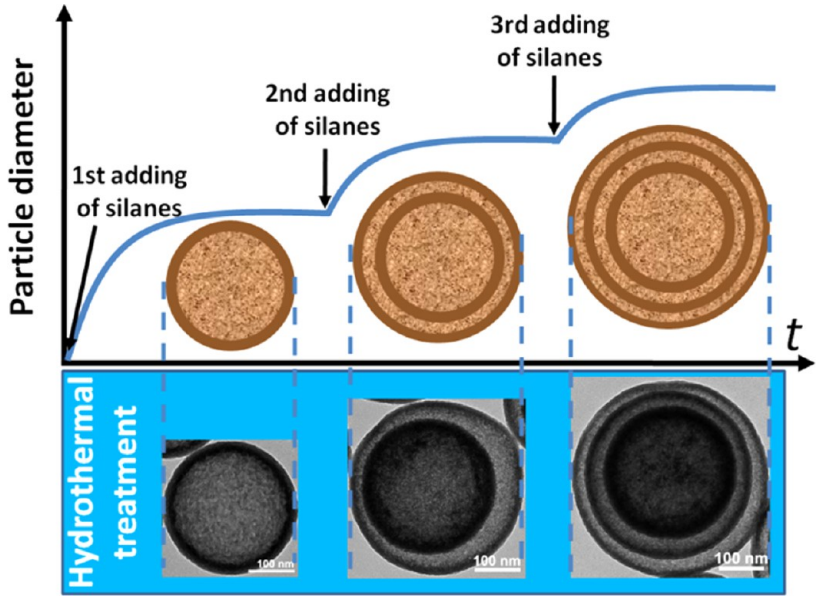

Figure 7. Schematic illustration of the successive growth process of the organosilica/CTAB composite spheres in ammonia and ethanol solution and the corresponding multi-shelled products after the hydrothermal treatment.

growth times were isolated and then hydrothermally treated. TEM images show that the diameter of the organosilica/CTAB spheres increases from 230 to 270 nm and then up to a final size of 300 nm with growth times of 10 min, 30 min, and 1 h (Supporting Information, Figure S9). Notably, the diameters of organosilica/CTAB composite spheres obtained at 10 and 30

DOI: 10.1021/jacs.5b05369
J. Am. Chem. Soc. 2015, 137, 7935–7944

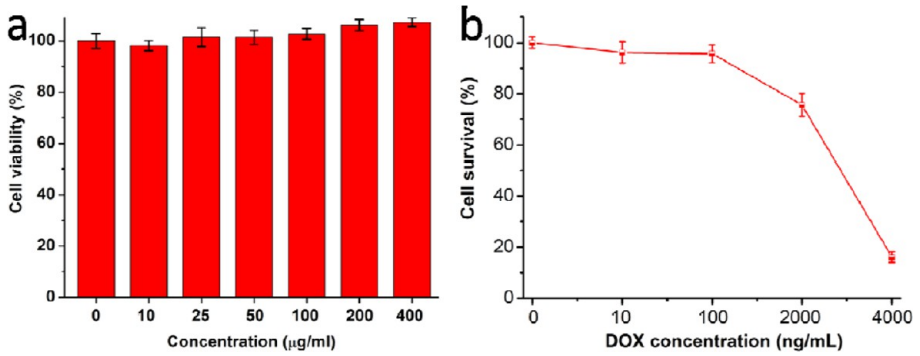

Figure 8. (a) *In vitro* viability of human embryo kidney 293 cells incubated with the triple-shelled PMO hollow spheres at different concentrations. (b) *In vitro* cytotoxicity of the triple-shelled PMO hollow spheres loaded with DOX on human breast adenocarcinoma cells for 48 h.

min are decreased to 194 and 254 nm after the hydrothermal treatment, and no hollow structures are observed. In contrast, hollow spheres are clearly present and the diameters of the organosilica/CTAB spheres grown for more than 1 h are well retained, clearly suggesting that the surfaces formed at later reaction stages are relatively stable. Thus, the growth of the organosilica/CTAB composite spheres via successive addition of silane precursors into the ammonia and ethanol solution can proceed as illustrated in Figure 7. Briefly, when silane precursors are added to the reaction solution, they are gradually hydrolyzed and condensed on the CTAB micelles to form mesostructured spherical particles. As the reaction proceeds, the diameter of the organosilica/CTAB composite spheres is gradually increased until almost all silicate species are exhausted. In the following processing time, the size of the organosilica/CTAB spheres does not change. However, the outer surfaces of the organosilica spheres can still contact the reaction solution, which contains a large amount of catalytic ammonia. Thus, the Si−OH and Si−OC_2H_5 groups on the surfaces can further be hydrolyzed and cross-linked to form a highly condensed layer. The ammonia-catalyzed cross-linking of Si−OH and Si−OC_2H_5 groups on the outer layers is dependent on the reaction temperature. Increasing the reaction temperature can accelerate the cross-linking and favor formation of thick, highly condensed organosilica layers. With the further addition of silane precursors into the reaction solution, more organosilica/CTAB layers with highly condensed surfaces are deposited on the pre-formed particles through repetition of the sol−gel process. Thus, mesostructured organosilica/CTAB composite spheres with multiple highly cross-linked interfaces are obtained. When the as-made organosilica/CTAB spheres are dispersed in water and hydrothermally treated, the organosilica/CTAB species with a low degree of condensation are attacked by water and dissolved. At the same time, the multiple interfaces with a high degree of condensation act as the nucleation centers for re-organization of the dissolved organosilica/CTAB composites. Thus, the condensation degree of the organosilica/CTAB spheres is increased and their framework's volume is shrunk toward the multiple interfaces, and multi-shelled hollow structures are eventually formed. Thanks to the highly controllable CTAB-directed sol−gel process, the diameter, inter-shell spacing, shell thickness, and organic group of the multi-shelled PMO hollow spheres can be facilely and precisely modulated by adjusting the reaction parameters.

Because they possess ordered mesopores and organic groups, PMOs have recently been explored as effective drug delivery carriers to fight against various kinds of diseases.[42] To illustrate the potential applications of the PMO hollow spheres in biomedical fields, the biocompatibility of the materials was assessed with human embryo kidney 293 cells. It is observed that the cell viability is retained 100% when they are incubated with the triple-shelled PMO hollow spheres at a concentration of 10−400 $\mu g\ mL^{-1}$ for 24 h (Figure 8a), which indicates a good biocompatibility of the materials. Next, DOX, a model chemotherapeutic drug used to treat a wide spectrum of cancers, was loaded into the PMO hollow spheres to prepare an anti-cancer drug delivery system. The loading efficiency of DOX in the triple-shelled PMO hollow spheres is measured to be 87 mg of DOX per milligram of PMOs. The anti-cancer effect of the drug delivery system was assessed in human breast adenocarcinoma (MDA-MB-231) cells. After co-incubation of MDA-MB-231 cells with different concentration of DOX-loaded PMOs for 48 h, the cancer cells are effectively killed by the DOX-loaded PMOs, and the cell survival was down to 16% at a DOX concentration of 4 $\mu g\ mL^{-1}$ (Figure 8b), indicating their excellent anti-cancer effect. Besides, because the multi-shelled PMO hollow spheres also have large cavities, the less water-soluble PFP gas can penetrate into the hollow spaces via the mesochannels. Through hydrophilic/hydrophobic interaction with the organic groups of the PMOs, the PFP can stay in the multi-shelled PMO hollow spheres to generate bubble contrast agents for ultrasound imaging. As shown in Supporting Information, Figure S10, the ultrasound signals of the PFP-filled PMO hollow spheres increase with the concentration of the contrast agents. Remarkably, the ultrasound signals can still be detected when the concentration of the contrast agents is only 0.6 $mg\ mL^{-1}$. The contrast-enhanced ultrasound imaging of the PFP-filled PMOs is significantly better than that of PFP-filled hollow mesoporous silicas due to their unique structure and hybrid frameworks.[43] These results suggest the potential of the multi-shelled PMO hollow spheres for biomedical applications.

4. CONCLUSIONS

In summary, we have demonstrated a simple and efficient multiple-interface transformation strategy to fabricate monodispersed multi-shelled PMO hollow spheres with controllable diameter (300−550 nm). This intrinsically simple strategy was implemented by a one-step hydrothermal treatment of successively grown organosilica spheres, which does not need any sacrificial templates or corrosive etching agents. The number (1−4) of the shells of the multi-shelled PMO hollow spheres can be accurately controlled by adjusting the addition

DOI: 10.1021/jacs.5b05369
J. Am. Chem. Soc. 2015, 137, 7935−7944

times of silane precursors. Also, the multi-shelled PMO hollow spheres possess a high surface area (~805 m^2/g), large pore volume (1.0 cm^3/g), radially oriented mesochannels (3.2 nm), inorganic−organic hybrid frameworks, and tunable shell thickness (10−30 nm) and chamber size (4−54 nm). In addition, alkyl, aromatic, and heteroelement fragments and their mixtures are successfully incorporated into the multi-shelled PMO hollow spheres, and their distribution can be controlled. The formation mechanism of the multi-shelled PMO hollow structures is ascribed to the outer surfaces of the organosilica frameworks formed in ammonia and ethanol solutions having a higher degree of cross-linking than the insides, which act as nucleation centers for re-organization of the organosilica frameworks during hydrothermal treatment. Cytotoxicity assay further confirms that the multi-shelled PMO hollow spheres possess excellent biocompatibility. Because the spheres possess accessible mesopores, the anti-cancer drug DOX can be loaded into the PMO hollows to construct an efficient delivery system, which shows remarkable cytotoxicity for human breast adenocarcinoma (MDA-MB-231) cells. In addition, thanks to the unique structure and hybrid frameworks, contrast agents can be successively constructed by loading PFP gas into the multi-shelled PMO hollow spheres. As a great variety of bridged silanes are available, they can also be combined with different materials through the sol−gel processes, and thus the strategy is expected to open up a novel and versatile route for synthesis of various sophisticated PMOs for multiple applications, such as separation, catalysis, energy conversion, etc.

■ ASSOCIATED CONTENT

Supporting Information

Additional SEM and TEM images, XRD pattern, and *in vitro* ultrasound imaging. The Supporting Information is available free of charge on the ACS Publications website at DOI: 10.1021/jacs.5b05369.

■ AUTHOR INFORMATION

Corresponding Authors

*dyzhao@fudan.edu.cn

*cjr.luguangming@vip.163.com

Author Contributions

#Z.T. and X.S. contributed equally.

Notes

The authors declare no competing financial interest.

■ ACKNOWLEDGMENTS

We greatly appreciate financial support from the National Key Basic Research Program of the PRC (2014CB744504, 2011CB707700, and 2013CB934104), the Major International (Regional) Joint Research Program of China (81120108013), the National Natural Science Foundation of China (30930028, 81201175, 81371611, and 21210004), the Natural Science Foundation of Jiangsu Province (BK20130863), and the National Science Foundation for Post-doctoral Scientists of China (2013T60939 and 2012M521934).

■ REFERENCES

(1) Schacht, S.; Huo, Q.; Voigt-Martin, I. G.; Stucky, G. D.; Schüth, F. *Science* **1996**, *273*, 768.

(2) Feyen, M.; Weidenthaler, C.; Schüth, F.; Lu, A.-H. *J. Am. Chem. Soc.* **2010**, *132*, 6791.

(3) Wang, B.; Chen, J. S.; Wu, H. B.; Wang, Z.; Lou, X. W. D. *J. Am. Chem. Soc.* **2011**, *133*, 17146.

(4) Ameloot, R.; Vermoortele, F.; Vanhove, W.; Roeffaers, M. B. J.; Sels, B. F.; Vos, D. E. D. *Nat. Chem.* **2011**, *3*, 382.

(5) Teng, Z.; Zheng, G.; Dou, Y.; Li, W.; Mou, C.-Y.; Zhang, X.; Asiri, A. M.; Zhao, D. *Angew. Chem., Int. Ed.* **2012**, *51*, 2173.

(6) Teng, Z.; Wang, S.; Su, X.; Chen, G.; Liu, Y.; Luo, Z.; Luo, W.; Tang, Y.; Ju, H.; Zhao, D.; Lu, G. *Adv. Mater.* **2014**, *26*, 3741.

(7) Yin, Y.; Rioux, R. M.; Erdonmez, C. K.; Hughes, S.; Somorjai, G. A.; Alivisatos, A. P. *Science* **2004**, *304*, 711.

(8) Huang, C.-C.; Huang, W.; Yeh, C.-S. *Biomaterials* **2011**, *32*, 556.

(9) Zhang, L.; Wu, H. B.; Lou, X. W. D. *J. Am. Chem. Soc.* **2013**, *135*, 10664.

(10) Wang, Z.; Zhou, L.; Lou, X. W. D. *Adv. Mater.* **2012**, *24*, 1903.

(11) Zhao, Y.; Jiang, L. *Adv. Mater.* **2009**, *21*, 3621.

(12) Xu, P.; Yu, R.; Ren, H.; Zong, L.; Chen, J.; Xing, X. *Chem. Sci.* **2014**, *5*, 4221.

(13) Dong, Z.; Lai, X.; Halpert, J. E.; Yang, N.; Yi, L.; Zhai, J.; Wang, D.; Tang, Z.; Jiang, L. *Adv. Mater.* **2012**, *24*, 1046.

(14) Dong, Z.; Ren, H.; Hessel, C. M.; Wang, J.; Yu, R.; Jin, Q.; Yang, M.; Hu, Z.; Chen, Y.; Tang, Z.; Zhao, H.; Wang, D. *Adv. Mater.* **2014**, *26*, 905.

(15) Xu, S.; Hessel, C. M.; Ren, H; Yu, R.; Jin, Q.; Yang, M.; Zhao, H.; Wang, D. *Energy Environ. Sci.* **2014**, *7*, 632.

(16) Wu, X.; Lu, G. Q. M.; Wang, L. *Energy Environ. Sci.* **2011**, *4*, 3565.

(17) Yang, Y.; Liu, X.; Li, X.; Zhao, J.; Bai, S.; Liu, J.; Yang, Q. *Angew. Chem., Int. Ed.* **2012**, *51*, 9164.

(18) Wong, Y.; Zhu, L.; Teo, W.; Tan, Y.; Yang, Y.; Wang, C.; Chen, H. *J. Am. Chem. Soc.* **2011**, *133*, 11422.

(19) Li, G.; Shi, Q.; Yuan, S. J.; Neoh, K. G.; Kang, E. T.; Yang, X. *Chem. Mater.* **2010**, *22*, 1309.

(20) Lee, J.; Hwang, S. H.; Yun, J.; Jang, J. *ACS Appl. Mater. Interfaces* **2014**, *6*, 15420.

(21) Li, W.; Deng, Y.; Wu, Z.; Qian, X.; Yang, J.; Wang, Y.; Gu, D.; Zhang, F.; Tu, B.; Zhao, D. *J. Am. Chem. Soc.* **2011**, *133*, 15830.

(22) Gu, D.; Bongard, H.; Deng, Y.; Feng, D.; Wu, Z.; Fang, Y.; Mao, J.; Tu, B.; Schüth, F.; Zhao, D. *Adv. Mater.* **2010**, *22*, 833.

(23) Liu, J.; Hartono, S. B.; Jin, Y. G.; Li, Z.; Lu, G. Q. M.; Qiao, S. Z. *J. Mater. Chem.* **2010**, *20*, 4595.

(24) Xu, H.; Wang, W. *Angew. Chem., Int. Ed.* **2007**, *46*, 1489.

(25) Yec, C. C.; Zeng, H. C. *Chem. Mater.* **2012**, *24*, 1971.

(26) Zhang, L.; Wang, H. *J. Phys. Chem. C* **2011**, *115*, 18479.

(27) Wang, Z.; Luan, D.; Li, C. M.; Su, F.; Madhavi, S.; Boey, F. Y. C.; Lou, X. W. *J. Am. Chem. Soc.* **2010**, *132*, 16271.

(28) Xiong, S.; Zeng, H. C. *Angew. Chem., Int. Ed.* **2012**, *51*, 949.

(29) Cho, W.; Lee, Y. H.; Lee, H. J.; Oh, M. *Adv. Mater.* **2011**, *23*, 1720.

(30) Lai, X.; Li, J.; Korgel, B. A.; Dong, Z.; Li, Z.; Su, F.; Du, J.; Wang, D. *Angew. Chem., Int. Ed.* **2011**, *50*, 2738.

(31) Brown, A. J.; Johnson, J. R.; Brunelli, N. A.; Koros, W. J.; Eum, K.; Jones, C. W.; Rashidi, F.; Nair, S. *Science* **2014**, *345*, 72.

(32) Park, S. S.; Moorthy, M. S.; Ha, C.-S. *NPG Asia Mater.* **2014**, *6*, e96.

(33) Asefa, T.; MacLachlan, M. J.; Coombs, N.; Ozin, G. A. *Nature* **1999**, *402*, 867.

(34) Van Der Voort, P.; Esquivel, D.; De Canck, E.; Goethals, F.; Van Driessche, I.; Romero-Salguero, F. J. *Chem. Soc. Rev.* **2013**, *42*, 3913.

(35) Teng, Z.; Su, X.; Lee, B.; Huang, C.; Liu, Y.; Wang, S.; Wu, J.; Xu, P.; Sun, J.; Shen, D.; Li, W.; Lu, G. *Chem. Mater.* **2014**, *26*, 5980.

(36) Djojoputro, H.; Zhou, X. F.; Qiao, S. Z.; Wang, L. Z.; Yu, C. Z.; Lu, G. Q. *J. Am. Chem. Soc.* **2006**, *128*, 6320.

(37) Chen, Y.; Xu, P.; Chen, H.; Li, Y.; Bu, W.; Shu, Z.; Li, Y.; Zhang, J.; Zhang, L.; Pan, L.; Cui, X.; Hua, Z.; Wang, J.; Zhang, L.; Shi, J. *Adv. Mater.* **2013**, *25*, 3100.

(38) Shopsowitz, K. E.; Hamad, W. Y.; MacLachlan, M. J. *J. Am. Chem. Soc.* **2012**, *134*, 867.

(39) Lu, D.; Lei, J.; Wang, L.; Zhang, J. *J. Am. Chem. Soc.* **2012**, *134*, 8746.

DOI: 10.1021/jacs.5b05369
J. Am. Chem. Soc. 2015, 137, 7935−7944

(40) Liu, J.; Yang, H. Q.; Kleitz, F.; Chen, Z. G.; Yang, T.; Strounina, E.; Lu, G. Q. M.; Qiao, S. Z. *Adv. Funct. Mater.* **2012**, *22*, 591.
(41) Chen, Y.; Meng, Q.; Wu, M.; Wang, S.; Xu, P.; Chen, H.; Li, Y.; Zhang, L.; Wang, L.; Shi, J. *J. Am. Chem. Soc.* **2014**, *136*, 16326.
(42) Croissant, J.; Cattoën, X.; Man, M. W. C.; Gallud, A.; Raehm, L.; Trens, P.; Maynadier, M.; Durand, J.-O. *Adv. Mater.* **2014**, *26*, 6174.
(43) Teng, Z.; Su, X.; Zheng, Y.; Sun, J.; Chen, G.; Tian, C.; Wang, J.; Li, H.; Zhao, Y.; Lu, G. *Chem. Mater.* **2013**, *25*, 98.

DOI: 10.1021/jacs.5b05369
J. Am. Chem. Soc. 2015, 137, 7935−7944